



<b>Title</b>	<b>Dislocation network at InN/GaN interface revealed by scanning tunneling microscopy</b>
<b>Author(s)</b>	<b>Liu, Y; Cai, Y; Zhang, L; Xie, MH; Wang, N; Zhang, SB; Wu, HS</b>
<b>Citation</b>	<b>Applied Physics Letters, 2008, v. 92 n. 23</b>
<b>Issued Date</b>	<b>2008</b>
<b>URL</b>	<b><a href="http://hdl.handle.net/10722/80858">http://hdl.handle.net/10722/80858</a></b>
<b>Rights</b>	<b>Creative Commons: Attribution 3.0 Hong Kong License</b>

## Dislocation network at InN/GaN interface revealed by scanning tunneling microscopy

Y. Liu,<sup>1</sup> Y. Cai,<sup>2</sup> Lixin Zhang,<sup>3</sup> M. H. Xie,<sup>1,a)</sup> N. Wang,<sup>2</sup> S. B. Zhang,<sup>3</sup> and H. S. Wu<sup>1</sup>

<sup>1</sup>Department of Physics, The University of Hong Kong, Pokfulam Road, Hong Kong, China

<sup>2</sup>Department of Physics, Hong Kong University of Science and Technology, Clear Water Bay, Kowloon, Hong Kong, China

<sup>3</sup>National Renewable Energy Laboratory, Golden, Colorado 80401, USA

(Received 7 May 2008; accepted 22 May 2008; published online 11 June 2008)

For heteroepitaxy of InN on GaN(0001) by molecular-beam epitaxy, the lattice misfit strain is relieved by misfit dislocations (MDs) formed at the interface between InN and GaN. Imaging by scanning tunneling microscopy (STM) of the surfaces of thin InN epilayers reveals line features parallel to  $\langle 11\bar{2}0 \rangle$ . Their contrast becomes less apparent for thicker epilayers. From the interline spacing as well as a comparison with transmission electron microscopy studies, it is suggested that they correspond to the MDs beneath the surface. The STM contrast originates from both the surface distortion caused by the local strain at MDs and the electronic states of the defects. © 2008 American Institute of Physics. [DOI: 10.1063/1.2944145]

Molecular-beam epitaxy (MBE) of InN on GaN represents a model heteroepitaxial system with large lattice mismatch and a huge difference in elastic constants. The epitaxial growth mode of InN on GaN(0001) has been studied previously, where both two-dimensional (2D) layer-by-layer mode and the Stranski–Krastanov (SK) mode of growth were observed, depending on the conditions of MBE.<sup>1</sup> In both 2D and SK growth, the relaxation of misfit strain was shown to be initiated by the formation of misfit dislocations (MDs) at the heterointerface between InN and GaN, which commences upon the completion of the first bilayer (1 BL  $\approx$  2.9 Å) InN deposition.<sup>1</sup> There have been a number of studies on the characteristics of the MDs in the InN/GaN heterosystem<sup>2–5</sup> where both 90° and 60° dislocations were noted.<sup>3–5</sup> There is also an inconsistency in terms of line directions of the dislocations, some suggested to be parallel to  $\langle 1\bar{1}00 \rangle$ ,<sup>3</sup> while others reported the  $\langle 11\bar{2}0 \rangle$  orientations.<sup>4,5</sup>

In a study of heteroepitaxial InAs on GaAs(111) by scanning tunneling microscopy (STM), MDs were revealed as dark lines in the STM images, where the surface contrast was explained by the elastic theory as due to surface distortion induced by the underlying dislocations.<sup>6</sup> A similar observation was made even earlier on the epitaxial system of CoSi<sub>2</sub>/Si(111).<sup>7</sup> These studies provided complementary information about dislocations, particularly at more local levels. Since STM can measure very small lattice distortion in the vertical direction, it allows an investigation of the material's elastic properties for ultrathin films.<sup>6–8</sup>

In this Letter, we report an observation of MD networks at InN/GaN(0001) heterointerface by STM. The dislocations are seen to be parallel to the  $\langle 11\bar{2}0 \rangle$  orientations. Separate transmission electron microscopy (TEM) examinations confirm the existence of the MDs being confined at the InN/GaN interface. The apparent “depths” and “width” of the dislocation lines in STM are measured, which reveal a film thickness dependence. The latter is consistent with the assignment that the line features in STM reflect the MDs at

the heterointerface rather than some *surface* superstructures. The measured interline spacing matches well the lattice misfit between InN and GaN ( $\sim 10\%$ ).

Film growth and subsequent surface characterizations of InN were carried out in a multichamber ultrahigh vacuum (UHV) system, where the MBE reactor and the STM chamber were connected via UHV interlocks. In MBE, besides the conventional Knudsen cells for metal gallium (Ga) and indium (In) sources, a radio-frequency plasma unit was employed for active nitrogen (N). Prior to InN deposition, a GaN buffer film was deposited on 6H-SiC(0001) substrate at  $\sim 620$  °C under the excess Ga condition (i.e., the flux ratio between Ga and N is greater than unity). Following an annealing procedure at 620 °C, by which the surface showed a transition from pseudo-(1  $\times$  1) to (2  $\times$  2),<sup>9</sup> the sample was cooled to 390–450 °C for subsequent InN deposition. For the latter, the flux ratio of In/N was  $\approx 1.5$  and the deposition rate was maintained at  $\sim 0.1$  BL/s.<sup>1</sup> During the whole deposition process, the surface was monitored *in situ* by reflection high-energy electron diffraction. Having deposited a specified thickness of InN, the sample was thermally quenched to room temperature by switching off the heating current flowing through the rectangular sample piece. It was then transferred under UHV to the adjacent STM chamber for surface characterizations. Constant current mode of STM was conducted at room temperature under the tunneling current of 0.1 nA and sample bias from  $-0.5$  to  $-2.5$  V. For a specifically grown sample, high resolution (HR) TEM experiments were carried out using a JEOL2010FEG TEM microscope operated at 200 keV. The cross sectional TEM specimen was prepared by standard mechanical thinning followed by argon ion milling.

Before presenting the STM and HRTEM results, we would like to mention that the initial GaN buffer films prepared by MBE on SiC(0001) substrate were of Ga polarity and atomically smooth, showing terraces and BL steps.<sup>10</sup> The postgrowth annealing was to desorb excess Ga adlayers from the surface as indicated by the appearance of the (2  $\times$  2) surface reconstruction.<sup>9</sup> For heteroepitaxial growth of InN on GaN(0001) under excess In, depending on substrate tempera-

<sup>a)</sup>Electronic mail: mhxie@hkusua.hku.hk.

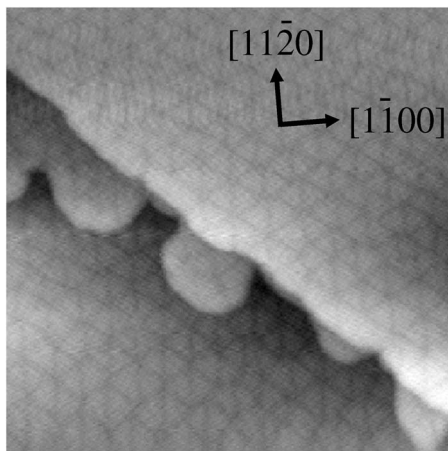


FIG. 1. STM image of the surfaces of an  $\sim 2$  BL InN film grown on GaN(0001). The sample bias of the STM was  $-2.5$  V. The image size is  $50 \times 50$  nm $^2$ .

ture, the deposition followed either the SK or 2D layer-by-layer modes,<sup>1</sup> but the following observation of the line features in STM applies to both cases.

Figure 1 presents a STM image of the surface of  $\sim 2$  BL InN film deposited on GaN(0001) at  $450^\circ\text{C}$ , where the growth mode was 2D.<sup>1</sup> A striking feature seen from the image is the presence of dark lines running parallel to  $\langle 11\bar{2}0 \rangle$ . These dark lines form a hexagonal network. The spacing between the neighboring parallel lines is measured to be around  $3.2$  nm, i.e., about ten lattice constants of GaN or nine lattice constants of InN ( $a_{\text{GaN}} \approx 3.18$  Å,  $a_{\text{InN}} \approx 3.54$  Å). This is consistent with the lattice misfit of the InN/GaN heterosystem.

As for the nature of these dark lines, it is first probable that they are surface features, representing, for example, a surface reconstruction where a missing row of In atoms effectively relieves the lattice misfit strain and the STM contrast simply reflects those missing atom rows. Indeed, strain induced surface reconstruction has been documented for Ge/Si(100) heteroepitaxial systems, where  $n \times 2$  (where  $n > 1$  is an integer) surface reconstruction was seen on the deposited Ge surface on Si.<sup>11</sup> On the other hand, due to the very thin epilayer thickness, these dark lines may instead reflect MDs below the surface, which are known to exist, relieving the lattice misfit strain in the crystal.<sup>12</sup> The MDs not only cause lattice distortion of surface atoms when the epilayer is not so thick, but also give rise to additional electronic density of states (DOS) of the surface. Both will give rise to the STM contrast seen in Fig. 1. In order to discriminate between the two possibilities, we have examined the layer

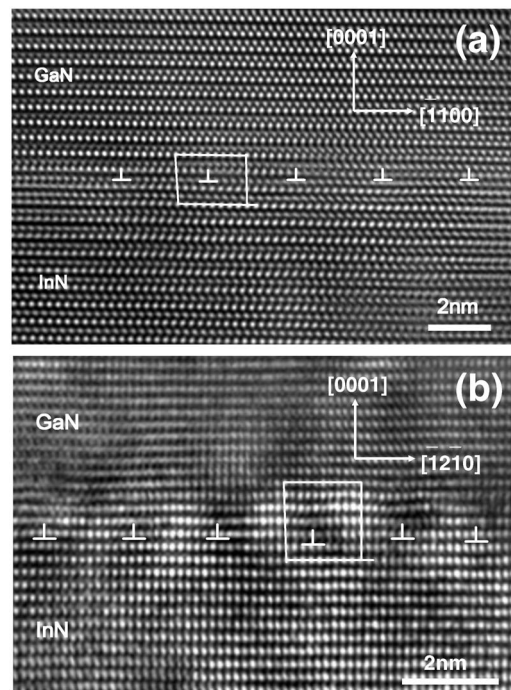


FIG. 3. HRTEM micrographs of InN/GaN interfaces viewed along (a)  $[11\bar{2}0]$  and (b)  $[10\bar{1}0]$ . The MDs are marked by “ $\perp$ ” and the Burgers circuits are also drawn.

thickness dependence of the line contrast. Figure 2 summarizes the depth and lateral width of the dark lines, measured from the line profiling of the STM, as functions of InN epilayer thickness. As seen, the lines appear shallower and wider as the epilayer gets thicker. These observations would favor dislocations over surface reconstruction for the observed dark lines by STM. For dislocations located at the heterointerface, with the increase in film thickness, the strain induced surface undulation becomes smaller in the vertical direction but more extended laterally.<sup>6</sup> The same can be said about the electronic contribution to surface DOS. As a result, the STM contrast will become weaker for thicker layers. If, on the other hand, they were surface features, the depth and width of the line features would not show a film thickness dependence.

To confirm that there are indeed arrays of MDs at the InN/GaN interface, we have examined a sample prepared under the same condition but for a greater thickness (for ease of TEM specimen preparation) by HRTEM. Figures 3(a) and 3(b) show cross-sectional HRTEM micrographs viewed along the  $[11\bar{2}0]$  and  $[10\bar{1}0]$  directions, respectively. From these, almost evenly spaced dislocations can be identified.

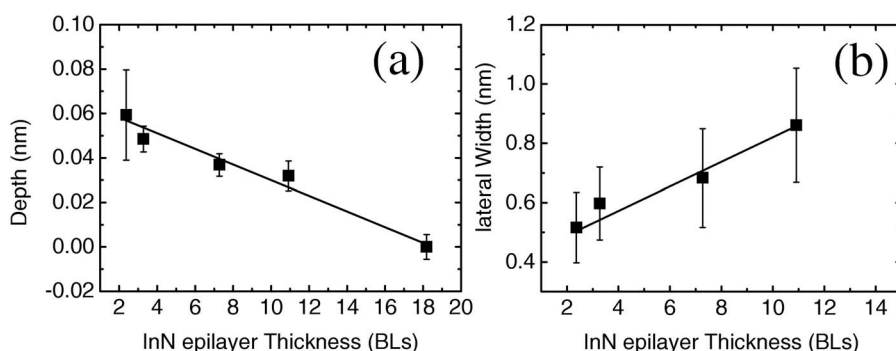


FIG. 2. The measured (a) depth and (b) lateral width of the dark lines for samples of different InN thicknesses. The lines are drawn to guide the eye, and the error bars represent the standard deviation of the mean.



However, if they are perfect  $60^\circ$  dislocations, a rhombus network at the heterointerface would be sufficient to relieve the misfit strains in all directions. However, such rhombus structures are rarely observed experimentally. Rather, we observe mostly hexagonal structures as shown in Fig. 1. To account for this, one may assume that the MDs are not all confined at the same InN/GaN interface plane but over an extended interface region. Due to the equivalence of the three  $\langle 11\bar{2}0 \rangle$  crystallographic directions on the (0001) plane, there can be differently oriented rhombus dislocation networks on different (but parallel) planes. When viewed atop from the surface, a hexagonal structure will show up. The TEM results shown in Fig. 3, however, do not seem to support this assignment. Instead, the MDs appear to all be confined at the very interface between InN and GaN. Furthermore, for the very thin layers we have examined (i.e., 2 BL), there is no extended interface region, yet hexagonal line networks are still observed.

We have recently carried out a theoretical investigation of the problem. Our studies reveal that the InN/GaN interface is comprised of three sets of  $90^\circ$  partial dislocations. They do not exist as uncorrelated network but have strong interaction with each other within the 2D plane to exhibit long-range order. The correlation of these dislocations comes from their formation mechanism. From Burgers circuit analysis we know that within one unit cell ( $9 \times 9$  InN/ $10 \times 10$  GaN) of the interface, there are two full MDs along the two principal axes of the (0001) plane. However, such an arrangement of dislocations contradicts the symmetry requirement of the interface. Based on the dissociation rule, each full dislocation ( $60^\circ$ ) can undergo a dissociation into two (one  $90^\circ$  and one  $30^\circ$ ) partial dislocations assisted by the formation of a low-energy stacking fault between the two partials. More importantly, the two  $30^\circ$  partial dislocations from different dissociations can further combine into a third  $90^\circ$  partial dislocation along the direction that is just symmetric to the two axes. Thus, at last, there are three sets of  $90^\circ$  partial dislocations which are strongly correlated and the symmetry of which is consistent with that of the interface. The interface structure with partial dislocations not only has lower strain energy due to the smaller Burgers vectors of the partial dislocations but also has minimum chemical energy by minimizing the number of dangling bonds within the dislocation cores. A more detailed account of the theoretical study is found in Ref. 13.

Finally, we show that electronic contribution to the STM contrast of the dislocations can be more important than topographic distortions of the surface. So one must be careful when extracting elastic data of the film from the measured lattice displacement by STM.<sup>6,7</sup> To illustrate this, in Fig. 4

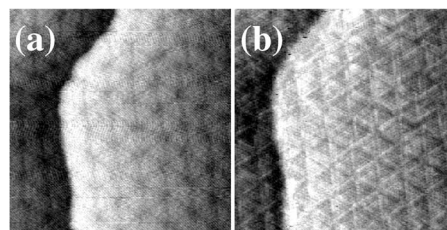


FIG. 4. STM images of an InN/GaN surface obtained at (a)  $-2.5$  V and (b)  $-0.5$  V. Note the contrast reversal of the dislocation lines in the two images (size:  $30 \times 30$  nm<sup>2</sup>).

we show two STM images of the same surface but obtained at different bias conditions. While in Fig. 4(a) the dislocations appear as dark lines similar to that of Fig. 1, in Fig. 4(b) the contrast is reversed, where the MDs show up as bright fringes when imaged at the bias of  $-0.5$  V. So even if the dislocations do induce surface lattice depressions, the local DOS on the surface as generated by the dislocations may well overcompensate lattice distortion.

In conclusion, MDs at the InN/GaN interface are observed by STM. These dislocations form hexagonal networks. The bias voltage dependence of the STM contrast suggests that additional electronic features are created on the surface by the MDs below.

This work is supported by the Research Grant Council of Hong Kong Special Administrative Region, China, under Grant Nos. HKU7047/05P and 7055/06P.

<sup>1</sup>Y. F. Ng, Y. G. Cao, M. H. Xie, X. L. Wang, and S. Y. Tong, *Appl. Phys. Lett.* **81**, 3960 (2002).

<sup>2</sup>G. Feuillet, B. Daudin, F. Widmann, J. L. Rouvière, and M. Arléry, *J. Cryst. Growth* **189/190**, 142 (1998).

<sup>3</sup>S. Srinivasan, L. Geng, R. Liu, F. A. Ponce, Y. Narukawa, and S. Tanaka, *Appl. Phys. Lett.* **83**, 5187 (2003).

<sup>4</sup>Th. Kehagias, A. Delimitis, Ph. Komninou, E. Iliopoulos, E. Dimakis, A. Georgakilas, and G. Nouet, *Appl. Phys. Lett.* **86**, 151905 (2005).

<sup>5</sup>C. J. Lu, X. F. Duan, Hai Lu, and W. J. Schaff, *J. Mater. Res.* **21**, 1693 (2006).

<sup>6</sup>J. G. Belk, J. L. Sudijono, X. M. Zhang, J. H. Neave, T. S. Jones, and B. A. Joyce, *Phys. Rev. Lett.* **78**, 475 (1997).

<sup>7</sup>R. Stalder, H. Sirringhaus, N. Onda, and H. von Känel, *Appl. Phys. Lett.* **59**, 1960 (1991).

<sup>8</sup>H. Yamaguchi, J. G. Belk, X. M. Zhang, J. L. Sudijono, M. R. Fahy, T. S. Jones, D. W. Pashley, and B. A. Joyce, *Phys. Rev. B* **55**, 1337 (1997).

<sup>9</sup>A. R. Smith, R. M. Feenstra, D. W. Greve, M.-S. Shin, M. Skowronski, J. Neugebauer, and J. E. Northrup, *J. Vac. Sci. Technol. B* **16**, 2242 (1998).

<sup>10</sup>S. M. Seutter, M. H. Xie, W. K. Zhu, L. X. Zheng, H. S. Wu, and S. Y. Tong, *Surf. Sci.* **445**, L71 (2000).

<sup>11</sup>R. Butz and S. Kamper, *Appl. Phys. Lett.* **61**, 1307 (1992).

<sup>12</sup>S. C. Jain, J. R. Willis, and R. Bullough, *Adv. Phys.* **39**, 127 (1990).

<sup>13</sup>L. Zhang, Y. Liu, Y. Cai, M. H. Xie, N. Wang, and S. B. Zhang (unpublished).